NEOPLASIA
www.neoplasia.com
Volume 26 Number xxx Month 2022 pp. 100779

Original Research

Myeloperoxidase exerts anti-tumor activity in glioma after radiotherapy

Muhammad Ali[a,b,c]; **Giulia Fulci**[a]; **Mantas Grigalavicius**[d]; **Benjamin Pulli**[a,e]; **Anning Li**[a]; **Gregory R. Wojtkiewicz**[a]; **Cuihua Wang**[a,e]; **Kevin Li-Chun Hsieh**[a]; **Jenny J. Linnoila**[a,f]; **Theodossis A. Theodossiou**[d]; **John W. Chen**[a,e,#]

[a] Institute for Innovation in Imaging and Center for Systems Biology, Massachusetts General Hospital, Harvard Medical School, Boston, Massachusetts, USA
[b] Department of Cancer Immunology, Institute for Cancer Research, Oslo University Hospital Radiumhospitalet, Oslo, Norway
[c] K.G. Jebsen Center for Cancer Immunotherapy, Institute of Clinical Medicine, University of Oslo, Norway
[d] Department of Radiation Biology, Institute for Cancer Research, Oslo University Hospital Radiumhospitalet, Oslo, Norway
[e] Department of Radiology, Massachusetts General Hospital, Boston, Massachusetts, USA
[f] Department of Neurology, Massachusetts General Hospital, Boston, Massachusetts, USA

Abstract

Background

Host immune response is a critical component in tumorigenesis and immune escape. Radiation is widely used for glioblastoma (GBM) and can induce marked tissue inflammation and substantially alter host immune response. However, the role of myeloperoxidase (MPO), a key enzyme in inflammation and host immune response, in tumorigenesis after radiotherapy is unclear. In this study, we aimed to determine how post-radiation MPO activity influences GBM and outcome.

Methods

We injected C57BL/6J or MPO-knockout mice with 005 mouse GBM stem cells intracranially. To observe MPO's effects on post-radiation tumor progression, we then irradiated the head with 10 Gy unfractionated and treated the mice with a specific MPO inhibitor, 4-aminobenzoic acid hydrazide (ABAH), or vehicle as control. We performed semi-quantitative longitudinal molecular MRI, enzymatic assays and flow cytometry to assess changes in inflammatory response and tumor size, and tracked survival. We also performed cell culture experiments in murine and human GBM cells to determine the effect of MPO on these cells.

Results

Brain irradiation increased the number of monocytes/macrophages and neutrophils, and boosted MPO activity by ten-fold in the glioma microenvironment. However, MPO inhibition dampened radiation-induced inflammation, demonstrating decreased MPO-specific signal on molecular MRI and attenuated neutrophil and inflammatory monocyte/macrophage recruitment to the glioma. Compared to saline-treated mice, both ABAH-treated and MPO-knockout mice had accelerated tumor growth and reduced survival. We further confirmed that MPO decreased tumor cell viability and proliferation in cell cultures.

Abbreviations: CNR, contrast-to-noise ratio; MPO, myeloperoxidase; ABAH, 4-aminobenzoic acid hydrazide; Ly-6C, Leukocyte antigen.

[#] Corresponding author.

Received 20 October 2021; received in revised form 16 February 2022; accepted 17 February 2022

https://doi.org/10.1016/j.neo.2022.100779

Conclusion

Local radiation to the brain initiated an acute systemic inflammatory response with increased MPO-carrying cells both in the periphery and the GBM, resulting in increased MPO activity in the tumor microenvironment. Inhibition or absence of MPO activity increased tumor growth and decreased host survival, revealing that elevated MPO activity after radiation has an anti-tumor role.

Neoplasia (2022) 26, 100779

Keywords: Glioblastoma (GBM), Myeloperoxidase, Radiation, Inflammation, Tumor microenvironment

Introduction

Glioblastoma (GBM) are devastating and highly lethal tumors [1,2]. These are the most common adult brain tumors and comprise a heterogeneous group of cells [3–5] with variable proliferating potential, transcriptional profile, areas of necrosis, hemorrhage and infiltration into normal brain parenchyma. Surgical debulking is difficult and almost all of the tumors recur from infiltrating tumor cells that escape surgical margins. GBM stem cells are particularly resistant to known therapies [6–8] and despite recent advancements in emerging molecular therapies [9], patient outcome has not improved significantly [10]. Median survival time is between 10 to 14.6 months with standard treatment [11,12] and the majority of patients die within 5 years of initial tumor diagnosis [13,14].

Radiotherapy is an essential component of standard treatment regimens for GBM [15]. After debulking surgery, patients undergo daily radiation treatment for 4 to 6 weeks. Radiation induces a significant host response, including direct DNA damage, reactive oxidation species formation [16], and cellular inflammation [17]. It can also prime antigen-presenting cells against tumor antigens [18] and initiate adaptive immune responses [19–21]. One of the key components of the host immune response is myeloperoxidase (MPO). MPO is a highly oxidative and inflammatory enzyme abundant in neutrophils and inflammatory monocytes (Ly-6C^{high}) [22], which infiltrate tumor margins [23]. MPO uses H_2O_2 as a substrate to generate a wide range of oxidative species, including converting Cl^- into hypochlorous acid (HOCl), a highly oxidizing agent [24]. MPO has been utilized experimentally as an imaging biomarker to differentiate therapy-induced inflammation from tumor recurrence [23]. The role of MPO in tumors is currently unclear, as it has been postulated to be both pro- [25,26] and anti-tumorigenic [27]. Although under chronic inflammatory conditions MPO promotes tumor growth [25], it is unknown what roles MPO plays in the context of the acute inflammation that follows radiation therapy. It is possible that by creating a highly oxidative and inflammatory microenvironment, MPO may be an important part of the innate immune response to help check tumor growth.

In this study, we investigated the role of MPO in radiation-induced inflammation and how MPO modulation affected tumor growth and survival in an immunocompetent mouse model of GBM stem cells [28]. This orthotopic syngeneic tumor model was chosen because the resultant tumor is pliable and infiltrates freely into the surrounding parenchyma with associated hemorrhage, necrosis, and loss of the blood-brain barrier – hallmarks of aggressive grade IV disease. We hypothesized that radiation recruits inflammatory myeloid cells and increases MPO enzymatic activity in the tumor microenvironment. Modulation of this elevated MPO activity could change tumor outcome and this knowledge could be utilized to generate future targeted therapies against GBM.

Methods

All protocols for animal experiments were approved by the Institutional Animal Care and Use Committee (IACUC) at Massachusetts General Hospital, Boston, MA and performed in accordance with the Declaration of Helsinki.

Animal models

8 to 12 weeks old wildtype male C57BL6/J mice (n=63, Jackson laboratories, RRID: IMSR_JAX:000664) and B6.129 × 1-Mpo^{tm1Lus}/J MPO knockout (MPO-KO) mice (n=5, Jackson laboratories, RRID: IMSR_JAX:004265) were used for the experiments. Intracranial tumors were induced using stereotactic brain injection in the right cerebral hemisphere. Briefly, mice were anesthetized with intraperitoneal pentobarbital (50mg/kg) and positioned on a stereotactic frame. A longitudinal incision was made in the skin and skull was exposed. A small burr hole was made 3 mm lateral to the sagittal suture and 2 mm caudal to the coronal suture. Care was taken to avoid visible blood vessels directly underneath the burr hole. Approximately 30,000 to 60,000 mouse 005 GBM stem cells (donated courtesy of Dr. Samuel D. Rabkin, MGH, Boston, MA) [28] in 2uL of PBS were slowly injected intracranially with a Hamilton syringe. After waiting 4-5 minutes to equilibrate intra-cranial pressures, the needle was then slowly removed and the burr hole was sealed with bone wax, followed by skin closure with sutures. For intra- and post-procedure analgesia, mice were injected with 0.1 mg/kg subcutaneous buprenorphine (Reckitt Benckiser Richmond, VA) twice daily for 2 days.

In vitro *cultures of the cell lines*

005 GBM stem cells were grown in DMEM F12 culture medium (Life technologies) supplemented with L-glutamine (2mM, CellGro), N2 supplement (1%, Gibco), human recombinant fibroblast growth factor-2 (20 ng/ml, PeproTech), human recombinant epidermal growth factor (20 ng/ml, R&D systems), and were routinely tested for mycoplasma contamination. For *in vitro* tumor sphere formation assay, 005 tumor spheroids were first dissociated into single cells with the help of 0.25% Trypsin-EDTA solution (Sigma-Aldrich). Cells were then cultured in complete media containing glucose oxidase in triplicates in the presence and absence of 1 U/mL of purified human MPO (Lee Biosolutions) for three to four days before being observed by microscopy.

LN18 and M059K human GBM cells were cultured using RPMI 1640 (Sigma-Aldrich) supplemented with 10% FCS (Thermo Fisher Scientific), 100 U/mL penicillin, 100 µg/mL streptomycin (Sigma-Aldrich), and 2mM L-Glutamine (Sigma-Aldrich) at 37°C in a 5% CO_2 humidified atmosphere. Cells were seeded into 96-well plates (Thermo Fisher Scientific) at a density

of 5000 cells/well for 12h before the incubation with 1U/mL MPO (Sigma-Aldrich) either in complete media or media containing 20% (v/v) of physiological NaCl solution (0.9%; Braun Melsungen AG). To analyze confluence as a surrogate for cell proliferation, the cells in the cultures were monitored by the IncuCyte® ZOOM live cell imaging system [29] (Essen Bioscience, Hertfordshire, UK). Cell proliferation was tracked for at least 72h. The confluence data is presented as a mean value of at least five parallel measurements ± standard error (SE). Cell viability was assessed by MTT assays at the end of MPO incubation period (72h) where all the solutions of the treatment phase were replaced by complete media containing 0.5mg/mL MTT (Sigma-Aldrich). The MTT containing media was replaced by 100uL/well of DMSO (Sigma-Aldrich) after 2h of incubation to dissolve formazan crystals. Finally, the absorbance measurements were performed at 561nm in the Tecan spark M10 plate reader. The viability data is presented as a mean value of at least five parallel measurements ± standard deviation (SD).

Mice irradiation

One or two weeks after tumor injection, mice heads were irradiated to mimic the systemic inflammatory response observed in post-irradiation clinical settings. Mice were anesthetized as described above and covered in lead plates such that only the cranium was exposed to the Cesium irradiation source. Mice were then irradiated with 10 Gy unfractionated to the head area and were randomized to different experimental groups. No mouse was excluded from the study. To investigate the post-irradiation effects of MPO inhibition, mice were intraperitoneally injected twice daily with 40 mg/kg of specific MPO inhibitor ABAH (4- Aminobenzoic acid hydrazide, Sigma), starting one hour after irradiation until the experimental endpoint and compared with saline injected mice as controls. For survival analysis of irradiated mice, data was pooled from two independent experiments.

In vivo *imaging*

To evaluate the effects of MPO inhibitor ABAH, we performed magnetic resonance imaging (MRI) with MPO-Gd (*bis*-5-hydroxytryptamide-diethylenetriaminepentaacetate-gadolinium) molecular MR agent two weeks after tumor irradiation. MPO-Gd is an activatable MR imaging agent that detects extracellular MPO activity *in vivo* with high specificity and sensitivity [30,31]. MPO-Gd was synthesized in our laboratory as previously described [32]. MR imaging was performed by using an animal 4.7-T MR imaging scanner (Bruker, Billerica, MA) before and after intravenous administration of MPO-Gd (0.3 mmol/kg). *In vivo* MPO activation was determined by calculating the activation ratio (ratio of contrast-to-noise ratios [CNRs] of lesions at delayed [60 minutes] and early [15 minutes] time points) [30]. Early enhancement represents leakage through blood-brain barrier breakdown, whereas delayed enhancement is derived mostly from agent retention caused by MPO activation [31].

To measure intracranial tumor growth non-invasively, mice were also imaged with the DTPA-Gd (diethylenetriaminepentaacetate-gadolinium) imaging agent one and two weeks after irradiation. Tumor bi-dimentional product (cm^2) was measured on axial post-contrast images by multiplying maximal tumor diameter to a second diameter drawn perpendicular to it (Macdonald's criteria [33]), and compared to those of ABAH-treated and MPO-KO mice. Both pre- and post-contrast enhanced T1 weighted images were acquired as previously described [23] and data were analyzed by investigators blinded to the experimental groups.

MPO activity assay

MPO enzymatic activity was measured in the irradiated tumors with modification of the protocol described previously [34] and compared to contra-lateral brain hemispheres without tumor as well as to non-irradiated tumor controls. To ensure that contralateral brains remained free of tumor, early radiation was performed on day 7 and mice were sacrificed on day 14 to measure MPO activity. Briefly, mice were transcardially perfused with 20 mL PBS containing 10 U/mL of Heparin. Brains were harvested and divided into two halves, (i) ipsi-lateral hemisphere with tumor and (ii) contra-lateral hemisphere without tumor. The halves were homogenized in a buffer containing 50mM of cetyl-trimethyl ammonium bromide (CTAB, Sigma-Aldrich) and 50mM of potassium phosphate, sonicated and centrifuged at 15,000 g to obtain the tissue extract. Tissue extracts were then diluted in MPO ELISA dilution buffer followed by incubation in anti-MPO antibody coated plates (Hycult Biotech, RRID: AB_10988477) for 1 hour at room temperature. After washing, MPO activity of captured MPO was assessed with a 10-acetyl-3,7-dihydroxyphenoxazine (ADHP, AAT Bioquest, Sunnyvale, CA) peroxidation assay and data was acquired on Safire 2 microplate reader (Tecan, Durham, NC) at an excitation wavelength of 535 nm and an emission wavelength of 590 nm [34]. Protein concentrations of the extracts were measured with a bicinchoninic acid assay kit (BCA; Thermo Scientific, Waltham, MA) and MPO activity was normalized and reported as relative fluorescence units (RFU)/sec/mg of proteins.

Flow cytometry

Flow cytometry was performed to quantify leukocyte subsets in non-irradiated and irradiated mice with and without ABAH treatment. Mice were sacrificed one week after radiation and tumor-carrying hemispheres were harvested for preparation of single cell suspensions. Briefly, tumor tissue was minced and passed through a cell 40 μm cell strainer. After washing, infiltrating leukocytes were separated for flow cytometry analysis by centrifugation through a discontinuous 30-70% percoll density gradient [35]. Peripheral blood was also collected through cardiac puncture and RBC lysis was performed to purify leukocytes. The following antibodies were used in the study: anti-CD45-APC (BD Bioscience, clone 30-F11, RRID: AB_398672); lineage cocktail [anti-CD90-PE, (BD Bioscience, clone 53-2.1, RRID: AB_394545); anti-NK1.1-P (BD Bioscience, clone PK136, RRID: AB_394677); anti-B220-PE (BD Bioscience, clone RA3-6B2, RRID: AB_10893353); anti-CD49b-PE (BD Bioscience, clone DX5, RRID: AB_395094); anti-TER-119-PE (BD Bioscience, clone TER-119, RRID: AB_394986)]; anti-CD11b-APC-Cy7 (BD Bioscience, clone M1/70, RRID: AB_396772); anti-Ly-6C-FITC (BD Bioscience, clone AL-21, RRID: AB_394628); anti-F4/80-PE-Cy7 (BD Bioscience, clone C1:A3-1) and biotin anti-Ly-6G (BioLegend, clone IA8, RRID:AB_1186108). A streptavidin-Pacific Orange conjugated secondary antibody was used for labeling biotinylated antibodies.

All leukocytes were identified as $CD45^+$, and myeloid cells as $(CD45^+)(Lin^{low}\ CD11b^{high})$. From the myeloid cell gate, neutrophils were identified as $[(Ly\text{-}6G^{high}\ Ly\text{-}6C^{int})(SSC^{int\text{-}high})]$ while $Ly\text{-}6C^{high}$ monocytes/macrophages (Mo/MΦ) in brain as $[(Ly\text{-}6G^{low}\ Ly\text{-}6C^{high}\ F4/80^{high})(SSC^{low})]$ and $Ly\text{-}6C^{high}$ monocytes in blood and bone marrow as $[(Ly\text{-}6G^{low}\ Ly\text{-}6C^{high}\ F4/80^{low})(SSC^{low})]$. The gating scheme utilized on tumor-infiltrating leukocytes is illustrated in **SI fig. 1**. Cell numbers of different cell populations were defined as total viable cell counts multiplied by the percentages of the respective sub-populations out of $CD45^+$ total leukocytes. Data for different leukocyte subsets were also reported as the percentage of total leukocytes ($CD45^+$). Data were acquired on a flow cytometer (LSR II; BD Biosciences, San Jose, CA) and analyzed with dedicated software (FlowJo, RRID: SCR_008520).

Statistical analysis

Results were reported as mean ± standard error of mean (SEM) unless otherwise stated. Unpaired student *t* test was utilized to compare normally

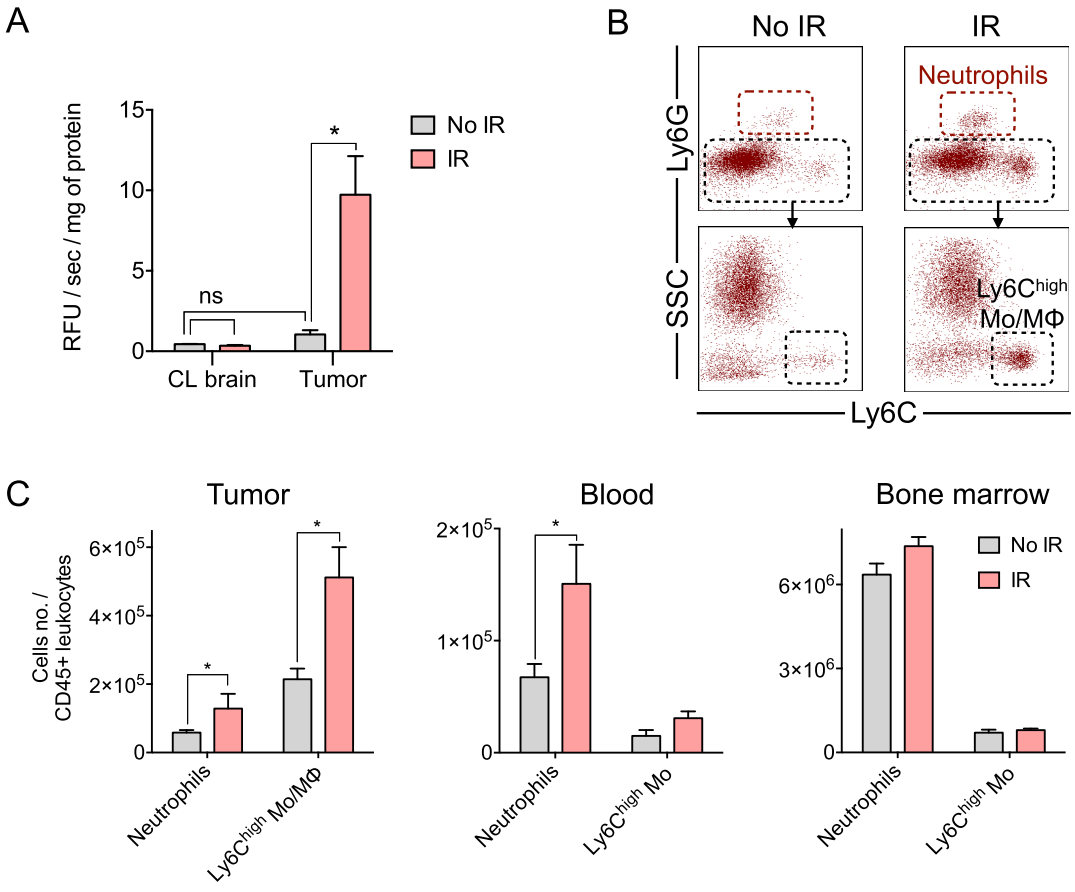

Fig. 1. Radiation increases MPO enzymatic activity and MPO carrying leukocytes in the tumor microenvironment. (A) Bar graphs showing increased MPO enzymatic activity measured as relative fluorescence units (RFU)/sec/mg of protein in irradiated (IR) tumors compared to non-irradiated (no IR) tumors. CL brain: contra-lateral normal cerebral hemisphere devoid of tumor. n = 4/group (B) Flow cytometry dot plots showing neutrophils and lymphocyte antigen 6C (Ly6C)^{high} monocytes/macrophage (Mo/MΦ) in irradiated (IR) and non-irradiated (no IR) tumors. SSC: side scatter, Ly6G: lymphocyte antigen 6G. (C) Flow cytometry analysis showing neutrophil and Ly-6C^{high} monocyte/macrophages (Mo/MΦ) or monocyte (Mo) cell numbers out of total leukocytes defined as CD45+ cells. Cells were isolated from brain tumor (left), peripheral blood (middle) and bone marrow (right) of irradiated (IR) and non-irradiated (no IR) mice (n = 4-5/group). Mice were irradiated 14 days after tumor injections and flow cytometry was performed 1 week after radiation. Data plotted as mean ± SEM. $^{*}p < 0.05$.

distributed independent data sets. Whenever appropriate, paired t-test was employed to compare non-independent variables. Nonparametric Mann-Whitney *U* test was employed to compare non-normally distributed data sets. One-way ANOVA with adjustment for multiple comparisons with Dunnett's post-test was performed to compare >2 groups. Survival analysis was performed by two-sided Log-rank (Mantel-Cox) test. $P < 0.05$ was considered to indicate a significant difference. All statistical analyses were performed with GraphPad Prism 6 (RRID: SCR_002798).

Results

Radiation increased MPO enzymatic activity and MPO carrying leukocytes in tumor microenvironment

Compared to the non-irradiated (no-IR) tumors, MPO activity increased markedly in the irradiated (IR) tumors ($P = 0.03$, Fig. 1A). Interestingly, this increased MPO activity was localized only to the irradiated tumor-carrying hemispheres. Contra-lateral normal hemispheres, although subjected to the same dose of radiation, had minimal MPO enzymatic activity, similar to non-irradiated tumors and normal tissues (Fig. 1A).

Next, we investigated the cellular source of MPO in the tumor microenvironment. MPO is expressed mainly in neutrophils and inflammatory Ly6C^{high} monocytes [22], and to a lesser extent in activated microglia and macrophages [36]. On flow cytometry analysis of irradiated tumors, we found significantly increased number of tumor-infiltrating neutrophils and inflammatory Ly6C^{high} Mo/MΦ cells ($P = 0.03$, Fig. 1B & C) compared to mouse tumors that did not receive radiation. Neutrophils and Ly6C^{high} monocytes were also increased in the peripheral blood of these mice ($P = 0.03$ and $P = 0.06$ respectively, Fig. 1C). It is important to mention that we did not observe any myeloablative effect with localized radiation to the head. Bone marrow myeloid cell numbers did not decrease one week after irradiation (Fig. 1C). However, CD11b^{pos} myeloid cell and neutrophil percentages relative to total white blood cells were significantly increased after radiation (SI Fig. 2).

MPO inhibition with ABAH ameliorated radiation-induced inflammation

ABAH is an irreversible and specific MPO inhibitor [37] that can cross the blood-brain barrier [38] and has been used to inhibit MPO enzymatic

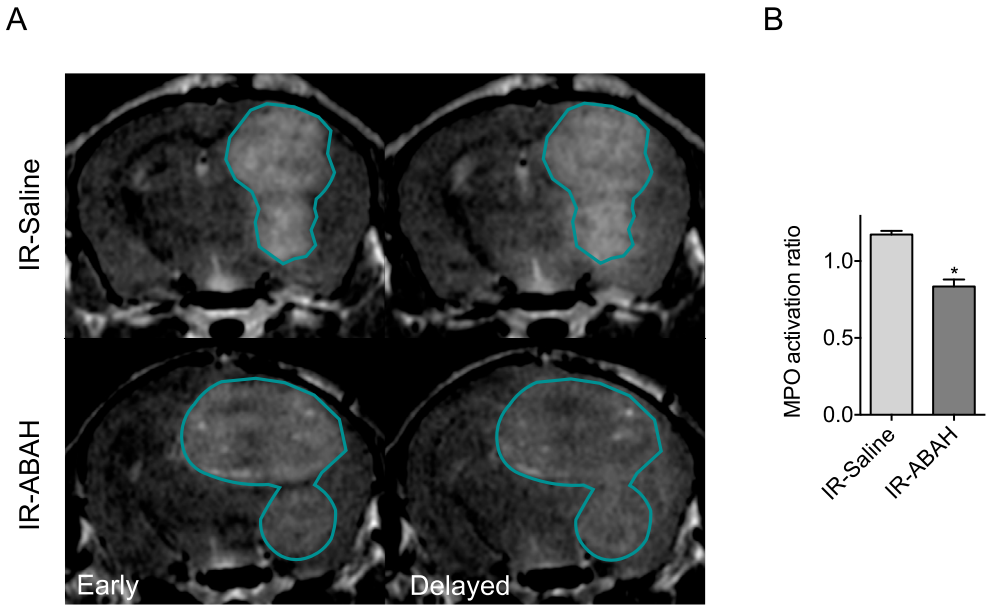

Fig. 2. Semi-quantitative measurement of *in-vivo* MPO inhibition by MPO-Gd MRI. *In vivo* MPO activity, measured by bis-5-hydroxytryptamide-diethylenetriaminepentaacetate-gadolinium (MPO-Gd) imaging, in tumor-bearing mice that were either injected with saline (IR-Saline) or the MPO-inhibitor 4-Aminobenzoic acid hydrazide (IR-ABAH) at two weeks after irradiation. (A) Representative axial T1-weighted images showing early (15 min) and delayed (60 min) contrast-enhanced images acquired after MPO-Gd injection; outlines highlight tumors in the brain (B) Bar graph showing MPO activation ratio of irradiated-tumors in saline (n = 2) and ABAH (n = 3) treated mice. MPO activation ratio was computed as a ratio of the contrast-to-noise ratios (CNRs) calculated from delayed (60 min) and early (15 min) post-contrast T1-weighted images. Data plotted as mean ± SEM. $^{*}p < 0.05$.

activity in various animal models of neuro-inflammatory diseases such as experimental autoimmune encephalitis [30], stroke [38], and epilepsy [39]. To document successful MPO inhibition in glioblastoma, we employed molecular MRI technology that spatially images as well as quantifies enzymatically active MPO *in situ* with the molecular contrast agent MPO-Gd (Fig. 2A). Compared to saline-injected mice, ABAH administration decreased MPO activation ratio, a marker of *in vivo* MPO activity [31] ($P = 0.03$, Fig. 2B), demonstrating successful partial inhibition of MPO, as reported previously [30,34,39].

Next, we sought to see if along with decreasing MPO activity, ABAH also affected the profile of the tumor-associated immune cells after irradiation. We found significantly decreased numbers of tumor-associated neutrophils ($p = 0.03$) and $Ly6C^{high}$ Mo/MΦ cells ($P = 0.047$, Fig. 3A & B) with ABAH administration compared to saline-injected mice. In peripheral blood, the total numbers of myeloid cells, particularly neutrophils and inflammatory monocytes, also decreased with ABAH administration (Fig. 3C). At the same time, bone marrow myeloid cells remained unchanged with ABAH treatment (Fig. 3D).

MPO inhibition or absence post-radiation promoted tumor growth

We next asked if this inhibition of radiation-induced inflammation and resultant changes in tumor-associated immune cells were simply a bystander effect or could they modulate the tumor microenvironment to be either pro-tumorigenic or anti-tumorigenic. To determine this, tumor-bearing wildtype and MPO-KO mice were irradiated and injected with either saline or ABAH (wildtype only) and imaged with MRI to quantify tumor size at one week (Fig. 4A & 4B, n = 4 mice/group) and 2 weeks (Fig. 4C, n = 5-9 mice/group) after radiation. To our surprise, two weeks of partial MPO inhibition with ABAH resulted in enhanced tumor cell growth, as bi-dimensional tumor product enlarged significantly compared to saline-injected mice (IR-Saline: 0.35 ± 0.06 cm^2, IR-ABAH: 0.59 ± 0.06 cm^2; $P = 0.01$, Fig. 4C). Additionally, this enhanced tumor growth was potentiated even more with the complete absence of MPO in MPO-KO mice. Two weeks after irradiation, tumor bi-dimensional product in irradiated MPO-KO mice was more than twice the size of saline-injected wildtype controls (IR-Saline: 0.35 ± 0.06 cm^2, IR-MPO-KO: 0.73 ± 0.08; $P = 0.003$, Fig. 4C).

MPO inhibition or absence post-radiation worsened survival

To correlate tumor size with clinical outcome, survival analysis was performed on irradiated saline- and ABAH-treated wildtype mice as well as on MPO-KO mice. As expected, irradiated mice survived longer than non-irradiated saline treated GBM-bearing mice (SI Fig. 3A, $P = 0.0006$). Similar to the tumor size quantification data, partial MPO inhibition with ABAH worsened survival compared to irradiated saline controls (median survival saline: 43 days vs. ABAH: 32 days, $P = 0.02$, Fig. 5A). MPO-KO mice also had worsened median survival compared to controls (saline: 43 days vs. MPO-KO: 32 days, $P = 0.005$, Fig. 5A & SI Fig. 3B), revealing that MPO plays an important role in post-radiation survival. Although median survival was similar in both ABAH-treated and MPO-KO mice, mice with complete MPO absence died earlier than mice with only partial MPO inhibition (Fig. 5A). Interestingly, an opposite effect was observed in non-irradiated, tumor-bearing wild-type mice with MPO inhibition. These mice, when treated with ABAH, showed an improved survival compared to those with saline treatment (Fig. 5B). As such, we did not observe a survival advantage between irradiated and non-irradiated ABAH treated groups, likely due to the opposing effects of the ABAH treatment on irradiated and non-irradiated mice (SI Fig. 3C). However, when we compared the irradiated saline-treated group to the non-irradiated but ABAH-treated group (SI Fig. 3D), we found the survival curves of the two groups were similar, implying that MPO inhibition without radiation may confer a similar survival benefit as radiation treatment.

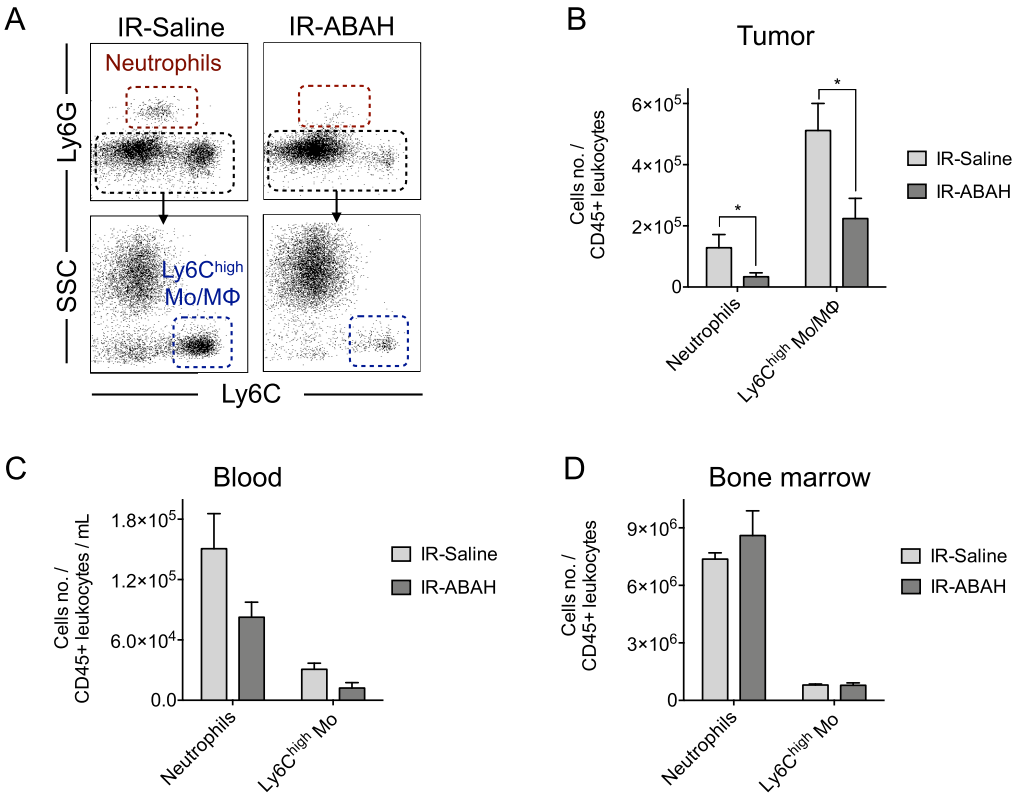

Fig. 3. MPO inhibition with ABAH decreased inflammatory cell recruitment. (A-D) Flow cytometry analysis showing neutrophil and Ly-6C^{high} monocyte (Mo) or monocytes/macrophage (Mo/MΦ) cell numbers out of total leukocytes defined as CD45+ cells, in brain tumor (A & B), peripheral blood (C) and bone marrow (D) of irradiated mice treated either with saline (IR-Saline) or ABAH (IR-ABAH) (n = 5/group). Mice were irradiated 14 days after tumor injections and flow cytometry was performed 1 week after radiation. SSC: side scatter, Ly6G: lymphocyte antigen 6G. Ly6C: lymphocyte antigen 6C. Data plotted as mean ± SEM. *p < 0.05.

Effect of MPO on cultured GBM cells

To further evaluate the effect of MPO on GBM, we conducted an *in vitro* cell culture study on 005 GBM stem cells. When these cells were cultured with MPO supplemented in culture media, we observed a stunted cell growth compared to untreated controls (Fig. 6A). This suggested that *in vitro* MPO has a potential anti-tumor role against GBM cells.

We also conducted experiments in two human GBM cell lines (LN18 and M059K) to assess the effect of exogenously administered MPO to the cell viability, using standard MTT assays (Fig. 6B & 6C). In the absence of NaCl, exogenously added MPO (1U/mL, 72h) did not have any effect on the cell viability in either of the two cell lines. When the media was supplemented with saline solution (NaCl), MPO decreased cell viability by ~32% in LN18 cells and ~28% in M059K cells ($P < 0.0001$). These results were further corroborated by complementary incuCyte experiments to assess proliferation. Control cells and MPO (1U/mL) treated cells in the presence of saline solution were placed in the IncuCyte® zoom, and left to grow for 72h. For both cell lines, a marked growth inhibition was observed in the presence of MPO (SI Fig. 4A & B). More specifically at the endpoint of 72h, there was a difference of 23% in the confluence of LN18 cells (77% without MPO, vs 54% with MPO), and a difference of 17% for M059K (49% without MPO, vs 32% with MPO). As expected, in the absence of saline solution to provide Cl^-, there was no significant difference in cell proliferation with/without MPO co-incubation (data not shown).

Discussion

The host immune response and the resultant tumor-associated immune microenvironment play important roles in tumorigenesis and immune escape. Myeloid cells can make up to 40% of the tumor mass. Our study showed that MPO, a key component of pro-inflammatory myeloid cell immune activity, plays an important role in the post-radiation inflammatory microenvironment. After irradiation, MPO activity was markedly elevated in the tumor microenvironment. Inhibiting or genetically removing MPO caused tumors to grow faster, probably by evading inflammatory and oxidative damage induced by radiation. Furthermore, *in vitro* cell-culture assays demonstrated that MPO can reduce GBM viability and reduce proliferation, confirming a role of MPO against GBM after radiation.

Our flow cytometry data showed that MPO inhibition post-radiation decreased myeloid cells in the tumor and in the blood, but not bone marrow. It is likely that by inhibiting MPO activity and thus decreasing oxidative stress and inflammation, there are decreased stimuli to recruit myeloid cells from the bone marrow to the blood and subsequently into the brain. However, while local radiation to the brain did not alter the number of myeloid cells in the bone marrow, the proportion of MPO-carrying cells (CD11b^{pos} myeloid cell and neutrophil) relative to total white blood cells significantly increased after radiation in the bone marrow (**SI fig. 2**). Taken together, these data revealed that localized brain tumor radiation initiated an acute systemic inflammatory response with increased MPO-carrying cells both in the periphery and in the tumor, resuling in increased MPO activity in the tumor microenvironment.

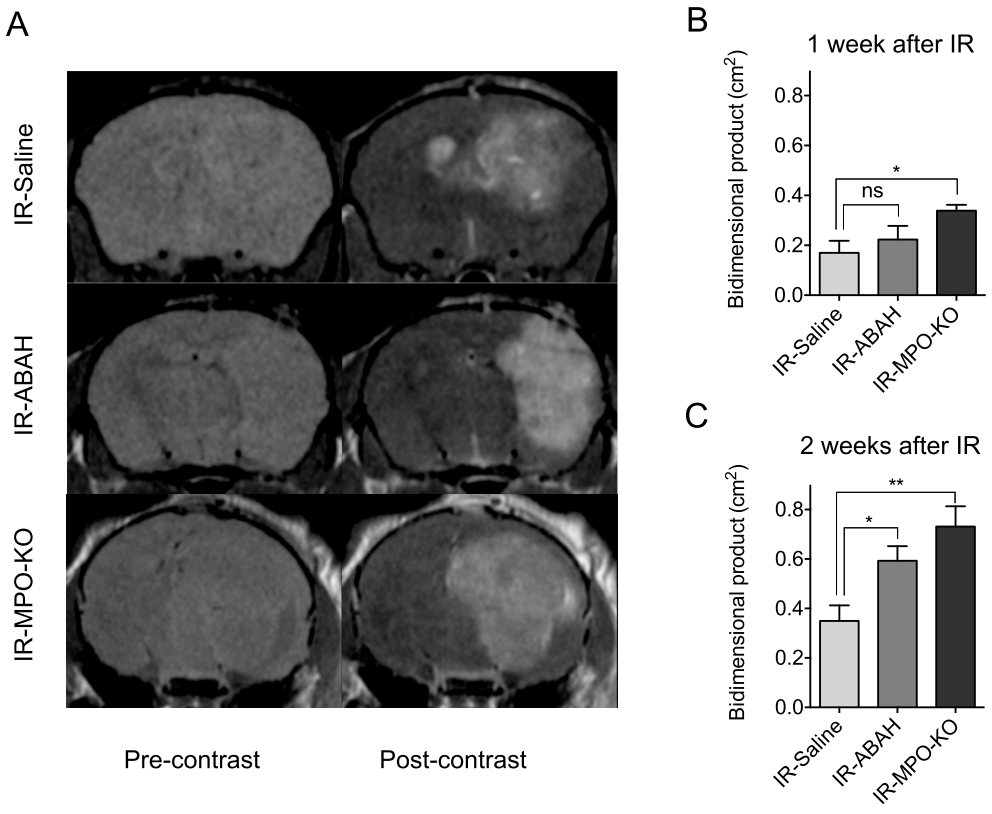

Fig. 4. MPO inhibition or absence post-radiation accelerated tumor growth. (A) Axial T1 weighted pre- and post-contrast diethylenetriaminepentaacetate-gadolinium (DTPA-Gd) enhanced images acquired from tumor bearing mice at 1 week after radiation. Experimental groups comprised of wild-type mice treated with saline (IR-Saline) or ABAH (IR-ABAH), and MPO-knock out mice (IR-MPO-KO group). (B-C) Tumor size measured as the bi-dimensional product (cm^2) at one week (B, n = 4/group) and two weeks (C, n = 5-9/group) after irradiation. Data plotted as mean ± SEM. $^*p < 0.05$, $^{**}p < 0.01$, ns = not significant.

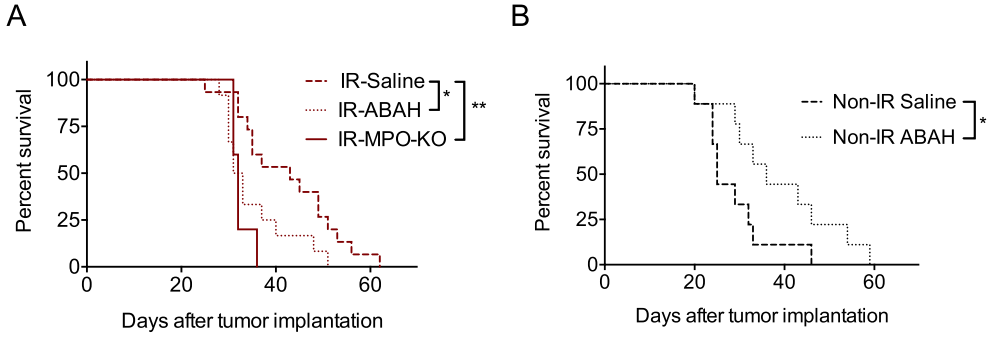

Fig. 5. Contrasting role of MPO inhibition on animal survival in irradiated and non-irradiated mice. (A) Survival analysis of the IR-Saline (n = 15), IR-ABAH (n = 12) and IR-MPO-KO (n = 5) mice groups. $^*p < 0.05$, $^{**}p < 0.01$ (B) Survival analysis of the saline and ABAH treated mice that were not irradiated (non-IR). Twice daily saline or ABAH injections were started from day 14 after tumor implantation. n = 9/group, $^*p < 0.05$.

GBM secretes factors that recruit and modify myeloid cells to create a microenvironment that facilitates tumor growth and invasion [40,41]. Within the tumor microenvironment, two dominant phenotypes have been identified: M1-like (classically activated, pro-inflammatory) cells and M2-like (alternatively activated, anti-inflammatory) cells [42]. M1-like cells are potent effector cells that kill microorganisms and tumor cells and produce large amounts of pro-inflammatory cytokines. In contrast, M2-like cells tune the inflammatory responses and adaptive Th1 immunity, scavenge debris, and promote angiogenesis, tissue remodeling and repair. A similar dichotomy exists for neutrophils with N1 (anti-tumor) and N2 (pro-tumor) polarization [43,44]. GBM hijacks inflammatory myeloid cells and generate signals that shift these myeloid cells toward the M2-like phenotype [45]. This tumor-driven plasticity appears not only in immune cells but also in immune effector molecules, such as MPO. In an experimental study on lung cancers that did not involve irradiation or any immune-enhancers [25], MPO inhibition or absence slowed tumor growth. Indeed, we observed similar results when GBM-bearing mice without prior irradiation that were treated with ABAH showed improved survival (Fig. 5B). In the context of chronic inflammation, MPO appeared to be detrimental for host-defense against tumor. Radiation, on the other hand, creates a highly oxidative and inflammatory milieu with

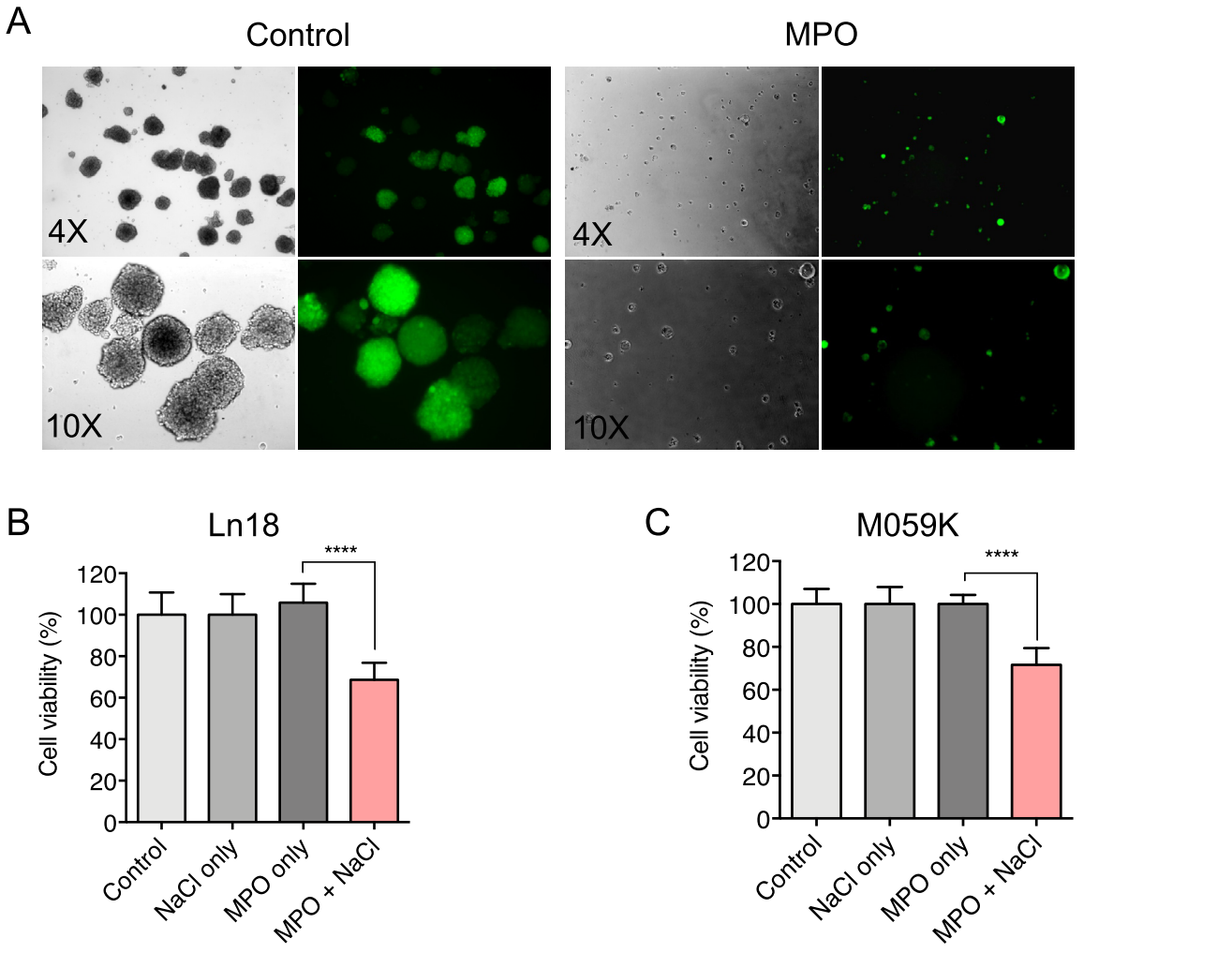

Fig. 6. Effect of MPO in *in vitro* cell-culture assays. (A) Representative images from *in vitro* cell cultures showing stunted cell proliferation after addition of active MPO in the culture media. Green fluorescence protein (GFP) expressing 005 GBM stem cells were used in the assays. Images were acquired with bright field and fluorescence microscopy for GFP at 4 times and 10 times magnification. (B-C) Bar graphs from cytotoxicity (MTT) assays on two human GBM cell lines Ln18 and M059K showing direct cytotoxic effects of MPO in media containing saline (NaCl).

10-fold more MPO activity compared to control normal brain (regardless of irradiation) and non-irradiated tumor-bearing brain (Fig. 1). In this environment, MPO appeared to shift to an anti-tumor role, likely by direct cytotoxic effect of MPO-induced oxidative damage [46].

Although in the *in vitro* cell cultures, important factors of tissue or cellular inflammatory cascades were not present, we still observed that in the presence of MPO and Cl^-, there was a substantial decrease in viability and proliferation in GBM cell lines. Interestingly, MPO can only induce cytotoxicity to the GBM cells when Cl^- is present, revealing that MPO induces cytotoxicity to GBM cells by its enzymatic activity to produce oxidants such as HOCl.

An important limitation of the study is that we used single radiation dose to induce tumor inflammation. Fractionated radiation dose regimen is the standard clinical practice to limit necrosis of the normal tissue. Interestingly, Boria et al. recently compared single high-dose radiation to a fractionated dose regimen in mice and did not find additional protection against radiation necrosis for the animals [47]. Based on this and because an unfractionated approach in rodents has practical advantages such as a shorter time commitment and avoidance of positioning errors from repetitive dosing that can affect reproducibility, we chose in this work to use a single high-dose. Nonetheless, future studies that employ this strategy would be desirable to better mimic the clinical experience. Another future direction would be a detailed histological examination of GBM tumor proliferation and its microenvironment under various conditions with and without MPO and irradiation. Our results (**SI fig. 3D**) also suggest that MPO inhibition without radiation may confer a similar survival benefit as radiation alone. It is possible that in this non-irradiated microenvironment, MPO inhibition may also act on immune cells in the tumor microenvironment. Thus, it would also be interesting to study how MPO and irradiation affect key immune cells in the tumor microenvironment, such as myeloid-derived suppressor cells that can block anti-tumor immunity in GBM patients [48,49].

Our study has two potentially important clinical implications for GBM management. First, new therapies may be explored that can enhance MPO driven inflammatory/oxidative damage in conjunction with radiotherapy. Second, the use of drugs that inhibit MPO (e.g. acetaminophen [50], isoniazid [51] and MPO-specific inhibitors in clinical development) may need to be further studied and possibly used with caution in GBM patients after radiotherapy.

Conclusion

In the acute inflammatory environment after radiation, our study identified an anti-tumor role for MPO in glioma progression. Irradiation increased both MPO enzymatic activity and MPO-secreting inflammatory cells in the tumor microenvironment. When this increased MPO was either partially inhibited or genetically absent, it resulted in accelerated tumor growth and consequently worsened survival. These results suggest that drugs that shift the immune response toward decreased MPO activity could limit the beneficial effects of radiotherapy, while strategies that maintain or increase MPO activity after radiotherapy may be new therapeutic directions.

Declaration of Competing interests

J.W.C. is a founder of Silverier and Einsenca. The other authors declare no competing financial interests.

Funding

National Institutes of Health (R01NS103998); National Multiple Sclerosis Society.

Authors' contributions

M.A. and J.W.C. conceived the idea. M.A., G.F., M.G., T.A.T., B.P., A.L., G.R.W., K.L.H., J.W.C. and J.J.L. designed and performed experiments, and analyzed the data. M.A., T.A.T. and J.W.C. wrote the manuscript. All authors revised the manuscripts critically and approved the final draft. J.W.C. supervised the study.

Acknowlegments

We thank Negin Jalali Motlagh for experimental assistance.

Supplementary materials

Supplementary material associated with this article can be found, in the online version, at doi:10.1016/j.neo.2022.100779.

References

[1] Louis DN, Perry A, Wesseling P, Brat DJ, Cree IA, Figarella-Branger D, Hawkins C, Ng HK, Pfister SM, Reifenberger G, et al. The 2021 WHO Classification of Tumors of the Central Nervous System: a summary. *Neuro-Oncology* 2021;**23**:1231–51.

[2] Omuro A, DeAngelis LM. Glioblastoma and other malignant gliomas: a clinical review. *JAMA* 2013;**310**:1842–50.

[3] Neftel C, Laffy J, Filbin MG, Hara T, Shore ME, Rahme GJ, Richman AR, Silverbush D, Shaw ML, Hebert CM, et al. An Integrative model of cellular states, plasticity, and genetics for glioblastoma. *Cell* 2019;**178**:835–49 e821.

[4] Richards LM, Whitley OKN, MacLeod G, Cavalli FMG, Coutinho FJ, Jaramillo JE, Svergun N, Riverin M, Croucher DC, Kushida M, et al. Gradient of Developmental and Injury Response transcriptional states defines functional vulnerabilities underpinning glioblastoma heterogeneity. *Nature Cancer* 2021;**2**:157–73.

[5] Castellan M, Guarnieri A, Fujimura A, Zanconato F, Battilana G, Panciera T, Sladitschek HL, Contessotto P, Citron A, Grilli A, et al. Single-cell analyses reveal YAP/TAZ as regulators of stemness and cell plasticity in glioblastoma. *Nat Cancer* 2021;**2**:174–88.

[6] Bao S, Wu Q, McLendon RE, Hao Y, Shi Q, Hjelmeland AB, Dewhirst MW, Bigner DD, Rich JN. Glioma stem cells promote radioresistance by preferential activation of the DNA damage response. *Nature* 2006;**444**:756–60.

[7] Bhaduri A, Di Lullo E, Jung D, Müller S, Crouch EE, Espinosa CS, Ozawa T, Alvarado B, Spatazza J, Cadwell CR, et al. Outer radial glia-like cancer stem cells contribute to heterogeneity of glioblastoma. *Cell Stem Cell* 2020;**26**:48–63 e46.

[8] Prager BC, Bhargava S, Mahadev V, Hubert CG, Rich JN. Glioblastoma stem cells: driving resilience through chaos. *Trends Cancer* 2020;**6**:223–35.

[9] Thomas AA, Brennan CW, DeAngelis LM, Omuro AM. Emerging therapies for glioblastoma. *JAMA Neurol* 2014;**71**:1437–44.

[10] Reardon DA, Brandes AA, Omuro A, Mulholland P, Lim M, Wick A, Baehring J, Ahluwalia MS, Roth P, Bähr O, et al. Effect of nivolumab vs bevacizumab in patients with recurrent glioblastoma: The CheckMate 143 Phase 3 Randomized Clinical Trial. *JAMA Oncol* 2020;**6**:1003–10.

[11] Stupp R, Mason WP, van den Bent MJ, Weller M, Fisher B, Taphoorn MJ, Belanger K, Brandes AA, Marosi C, Bogdahn U, et al. Radiotherapy plus concomitant and adjuvant temozolomide for glioblastoma. *N Engl J Med* 2005;**352**:987–96.

[12] Perry JR, Laperriere N, O'Callaghan CJ, Brandes AA, Menten J, Phillips C, Fay M, Nishikawa R, Cairncross JG, Roa W, et al. Short-course radiation plus temozolomide in elderly patients with glioblastoma. *New Engl J Med* 2017;**376**:1027–37.

[13] Stupp R, Hegi ME, Mason WP, van den Bent MJ, Taphoorn MJ, Janzer RC, Ludwin SK, Allgeier A, Fisher B, Belanger K, et al. Effects of radiotherapy with concomitant and adjuvant temozolomide versus radiotherapy alone on survival in glioblastoma in a randomised phase III study: 5-year analysis of the EORTC-NCIC trial. *Lancet Oncol* 2009;**10**:459–66.

[14] Poon MTC, Sudlow CLM, Figueroa JD, Brennan PM. Longer-term (≥ 2 years) survival in patients with glioblastoma in population-based studies pre- and post-2005: a systematic review and meta-analysis. *Scient Rep* 2020;**10**:11622.

[15] Barani IJ, Larson DA. Radiation therapy of glioblastoma. *Cancer Treat Res* 2015;**163**:49–73.

[16] Diehn M, Cho RW, Lobo NA, Kalisky T, Dorie MJ, Kulp AN, Qian D, Lam JS, Ailles LE, Wong M, et al. Association of reactive oxygen species levels and radioresistance in cancer stem cells. *Nature* 2009;**458**:780–3.

[17] Tabatabaei P, Visse E, Bergstrom P, Brannstrom T, Siesjo P, Bergenheim AT. Radiotherapy induces an immediate inflammatory reaction in malignant glioma: a clinical microdialysis study. *J Neurooncol* 2016.

[18] Klug F, Prakash H, Huber PE, Seibel T, Bender N, Halama N, Pfirschke C, Voss RH, Timke C, Umansky L, et al. Low-dose irradiation programs macrophage differentiation to an iNOS(+)/M1 phenotype that orchestrates effective T cell immunotherapy. *Cancer Cell* 2013;**24**:589–602.

[19] Patel RB, Hernandez R, Carlson P, Grudzinski J, Bates AM, Jagodinsky JC, Erbe A, Marsh IR, Arthur I, Aluicio-Sarduy E, et al. Low-dose targeted radionuclide therapy renders immunologically cold tumors responsive to immune checkpoint blockade. *Science translational medicine* 2021;**13**.

[20] Herrera FG, Ronet C, Ochoa de Olza M, Barras D, Crespo I, Andreatta M, Corria-Osorio J, Spill A, Benedetti F, Genolet R, et al. Low-dose radiotherapy reverses tumor immune desertification and resistance to immunotherapy. *Cancer Discovery* 2022;**12**:108–33.

[21] Demaria S, Golden EB, Formenti SC. Role of Local Radiation Therapy in Cancer Immunotherapy. *JAMA Oncol* 2015;**1**:1325–32.

[22] Pulli B, Bure L, Wojtkiewicz GR, Iwamoto Y, Ali M, Li D, Schob S, Hsieh KL, Jacobs AH, Chen JW. Multiple sclerosis: myeloperoxidase immunoradiology improves detection of acute and chronic disease in experimental model. *Radiology* 2015;**275**:480–9.

[23] Kleijn A, Chen JW, Buhrman JS, Wojtkiewicz GR, Iwamoto Y, Lamfers ML, Stemmer-Rachamimov AO, Rabkin SD, Weissleder R, Martuza RL, et al. Distinguishing inflammation from tumor and peritumoral edema by myeloperoxidase magnetic resonance imaging. *Clin Cancer Res* 2011;**17**:4484–93.

[24] van der Veen BS, de Winther MP, Heeringa P. Myeloperoxidase: molecular mechanisms of action and their relevance to human health and disease. *Antioxid Redox Signal* 2009;**11**:2899–937.

[25] Rymaszewski AL, Tate E, Yimbesalu JP, Gelman AE, Jarzembowski JA, Zhang H, Pritchard KA Jr, Vikis HG. The role of neutrophil myeloperoxidase in models of lung tumor development. *Cancers (Basel)* 2014;**6**:1111–27.

[26] Wheatley-Price P, Asomaning K, Reid A, Zhai R, Su L, Zhou W, Zhu A, Ryan DP, Christiani DC, Liu G. Myeloperoxidase and superoxide dismutase polymorphisms are associated with an increased risk of developing pancreatic adenocarcinoma. *Cancer* 2008;**112**:1037–42.

[27] Droeser RA, Hirt C, Eppenberger-Castori S, Zlobec I, Viehl CT, Frey DM, Nebiker CA, Rosso R, Zuber M, Amicarella F, et al. High myeloperoxidase positive cell infiltration in colorectal cancer is an independent favorable prognostic factor. *PLoS One* 2013;**8**:e64814.

[28] Marumoto T, Tashiro A, Friedmann-Morvinski D, Scadeng M, Soda Y, Gage FH, Verma IM. Development of a novel mouse glioma model using lentiviral vectors. *Nat Med* 2009;**15**:110–16.

[29] Single A, Beetham H, Telford BJ, Guilford P, Chen A. A comparison of real-time and endpoint cell viability assays for improved synthetic lethal drug validation. *J Biomol Screening* 2015;**20**:1286–93.

[30] Forghani R, Wojtkiewicz GR, Zhang Y, Seeburg D, Bautz BR, Pulli B, Milewski AR, Atkinson WL, Iwamoto Y, Zhang ER, et al. Demyelinating diseases: myeloperoxidase as an imaging biomarker and therapeutic target. *Radiology* 2012;**263**:451–60.

[31] Breckwoldt MO, Chen JW, Stangenberg L, Aikawa E, Rodriguez E, Qiu S, Moskowitz MA, Weissleder R. Tracking the inflammatory response in stroke in vivo by sensing the enzyme myeloperoxidase. *Proc Natl Acad Sci U S A* 2008;**105**:18584–9.

[32] Chen JW, Querol Sans M, Bogdanov A Jr, Weissleder R. Imaging of myeloperoxidase in mice by using novel amplifiable paramagnetic substrates. *Radiology* 2006;**240**:473–81.

[33] Macdonald DR, Cascino TL, Schold SC Jr, Cairncross JG. Response criteria for phase II studies of supratentorial malignant glioma. *J Clin Oncol* 1990;**8**:1277–80.

[34] Pulli B, Ali M, Forghani R, Schob S, Hsieh KL, Wojtkiewicz G, Linnoila JJ, Chen JW. Measuring myeloperoxidase activity in biological samples. *PLoS One* 2013;**8**:e67976.

[35] Pino PA, Cardona AE. Isolation of brain and spinal cord mononuclear cells using percoll gradients. *J Vis Exp* 2011.

[36] Gray E, Thomas TL, Betmouni S, Scolding N, Love S. Elevated activity and microglial expression of myeloperoxidase in demyelinated cerebral cortex in multiple sclerosis. *Brain Pathol (Zurich, Switzerland)* 2008;**18**:86–95.

[37] Kettle AJ, Gedye CA, Winterbourn CC. Mechanism of inactivation of myeloperoxidase by 4-aminobenzoic acid hydrazide. *Biochem J* 1997;**321**(Pt 2):503–8.

[38] Forghani R, Kim HJ, Wojtkiewicz GR, Bure L, Wu Y, Hayase M, Wei Y, Zheng Y, Moskowitz MA, Chen JW. Myeloperoxidase propagates damage and is a potential therapeutic target for subacute stroke. *J Cereb Blood Flow Metab* 2015;**35**:485–93.

[39] Zhang Y, Seeburg DP, Pulli B, Wojtkiewicz GR, Bure L, Atkinson W, Schob S, Iwamoto Y, Ali M, Zhang W, et al. Myeloperoxidase Nuclear Imaging for Epileptogenesis. *Radiology* 2016;**278**:822–30.

[40] Kolaczkowska E, Kubes P. Neutrophil recruitment and function in health and inflammation. *Nat Rev Immunol* 2013;**13**:159–75.

[41] Shi C, Pamer EG. Monocyte recruitment during infection and inflammation. *Nat Rev Immunol* 2011;**11**:762–74.

[42] Sica A, Larghi P, Mancino A, Rubino L, Porta C, Totaro MG, Rimoldi M, Biswas SK, Allavena P, Mantovani A. Macrophage polarization in tumour progression. *Semin Cancer Biol* 2008;**18**:349–55.

[43] Houghton AM. The paradox of tumor-associated neutrophils: fueling tumor growth with cytotoxic substances. *Cell Cycle* 2010;**9**:1732–7.

[44] Magod P, Mastandrea I, Rousso-Noori L, Agemy L, Shapira G, Shomron N, Friedmann-Morvinski D. Exploring the longitudinal glioma microenvironment landscape uncovers reprogrammed pro-tumorigenic neutrophils in the bone marrow. *Cell Rep* 2021;**36**:109480.

[45] Sica A, Schioppa T, Mantovani A, Allavena P. Tumour-associated macrophages are a distinct M2 polarised population promoting tumour progression: potential targets of anti-cancer therapy. *Eur J Cancer* 2006;**42**:717–27.

[46] Pulli B, Ali M, Iwamoto Y, Zeller MW, Schob S, Linnoila JJ, Chen JW. Myeloperoxidase-Hepatocyte-Stellate Cell Cross Talk Promotes Hepatocyte Injury and Fibrosis in Experimental Nonalcoholic Steatohepatitis. *Antioxid Redox Signal* 2015;**23**:1255–69.

[47] Boria AJ, Perez-Torres CJ. Minimal difference between fractionated and single-fraction exposure in a murine model of radiation necrosis. *Radiat Oncol* 2019;**14**:144.

[48] Mi Y, Guo N, Luan J, Cheng J, Hu Z, Jiang P, Jin W, Gao X. The Emerging Role of Myeloid-Derived Suppressor Cells in the Glioma Immune Suppressive Microenvironment. *Front Immunol* 2020;**11**:737.

[49] Lakshmanachetty S, Cruz-Cruz J, Hoffmeyer E, Cole AP, Mitra SS. New Insights into the Multifaceted Role of Myeloid-Derived Suppressor Cells (MDSCs) in High-Grade Gliomas: From Metabolic Reprograming, Immunosuppression, and Therapeutic Resistance to Current Strategies for Targeting MDSCs. *Cells* 2021;**10**.

[50] Koelsch M, Mallak R, Graham GG, Kajer T, Milligan MK, Nguyen LQ, Newsham DW, Keh JS, Kettle AJ, Scott KF, et al. Acetaminophen (paracetamol) inhibits myeloperoxidase-catalyzed oxidant production and biological damage at therapeutically achievable concentrations. *Biochem Pharmacol* 2010;**79**:1156–64.

[51] Forbes LV, Furtmuller PG, Khalilova I, Turner R, Obinger C, Kettle AJ. Isoniazid as a substrate and inhibitor of myeloperoxidase: identification of amine adducts and the influence of superoxide dismutase on their formation. *Biochem Pharmacol* 2012;**84**:949–60.